Acta Crystallographica Section D
Biological Crystallography
ISSN 0907-4449

Using high-throughput *in situ* plate screening to evaluate the effect of dehydration on protein crystals

Alice Douangamath,[a]‡ Pierre Aller,[a]‡ Petra Lukacik,[a,b] Juan Sanchez-Weatherby,[a] Isabel Moraes[a,b,c] and Jose Brandao-Neto[a]*

[a]Life Science, Diamond Light Source, Harwell Science and Innovation Campus, Didcot, Oxfordshire OX11 0DE, England, [b]Research Complex at Harwell, Rutherford Appleton Laboratory, R92, Didcot, Oxfordshire OX11 0FA, England, and [c]Membrane Protein Laboratory, Imperial College, London SW7 2AZ, England

‡ These authors contributed equally to this work.

Correspondence e-mail: jose.brandao-neto@diamond.ac.uk

Received 22 October 2012
Accepted 23 January 2013

Crystal dehydration is a post-crystallization technique that can potentially improve the diffraction of macromolecular crystals. There are currently several ways of undertaking this process; however, dehydration experiments are often limited in their throughput and require prior manipulation of the samples. In the present study, a novel method is proposed that uses *in situ* plate screening to assess the effect of dehydration by combining the throughput of 96-well crystallization plates with direct X-ray feedback on crystal diffraction quality.

1. Introduction

Recently, *in situ* data collection from crystallization plates has greatly advanced both at home sources using the PX scanner (Agilent Technologies), G-Rob (NatXray) and Astra-Zeneca's plate-adaptor tool (Hargreaves, 2012) and at synchrotron facilities (Jacquamet *et al.*, 2004; Bingel-Erlenmeyer *et al.*, 2011; Mueller *et al.*, 2012; Axford *et al.*, 2012; Lobley *et al.*, 2012). The increased interest in *in situ* data collection has led to the further development of SBS-format crystallization plates to reduce X-ray scattering by the plastic and to increase the data-collection angle (CrystalQuickX, Greiner Bio-One; Soliman *et al.*, 2011). The technique has successfully been used to solve viral structures, where crystals could not be cryoprotected (Axford *et al.*, 2012), and in ligand-binding studies (le Maire *et al.*, 2011).

Dehydration is often achieved by simply exposing crystals to air. Several protocols for controlled experiments are available (Krauss *et al.*, 2012; Newman, 2006; Heras & Martin, 2005) in which the relative humidity of the surrounding air is gradually reduced using progressive exchange of the mother liquor with an increased gradient of desiccant solutions. During this process, molecules might undergo a small reorganization which could lead to altered unit-cell parameters and possibly to better diffraction (Efremov *et al.*, 2010; Umena *et al.*, 2011). Dehydration experiments by evaporation have the drawback of not being reproducible. This problem was overcome by the emergence of the Free Mounting System (FMS, Rigaku; Kiefersauer *et al.*, 2000) and the Humidity Controller Device (HC1b) at the European Synchrotron Radiation Facility (ESRF; Sanchez-Weatherby *et al.*, 2009; Russi *et al.*, 2011) which enabled accurate control of the relative humidity of samples, but only allowed one or two samples to be conditioned per experiment.

In this study, we have implemented a high-throughput procedure for undertaking dehydration experiments using the *in situ* plate-screening setup on beamline I04-1 at Diamond Light Source. We have applied it to a novel membrane-associated protein involved in K^+-channel regulation (details of the structure will be published elsewhere). This technique (used either in the home laboratory or at the synchrotron) avoids handling of the crystals and provides a direct X-ray assessment of the effect of dehydration for a broad range of conditions in a single experiment.

2. Methods and results

The membrane-associated protein could be reproducibly crystallized in space group $I422$ (unit-cell parameters $a = b = 107.4$, $c = 221.9$ Å) in

the presence of ammonium sulfate as the precipitant, but most of the crystals diffracted to 2.9 Å resolution or lower at the synchrotron. Further optimization trials did not improve the diffraction quality of these crystals.

For the dehydration experiment, the crystals were prepared in 96-well CrystalQuickX plates (Greiner Bio-One) using a Mosquito robot (TTP LabTech). 100 nl protein solution was mixed with 100 nl well solution and allowed to equilibrate against 30 µl well solution at 293 K for a week. A 96 deep-well block containing 20 increasing concentrations of sodium chloride from 0 to 5 *M* in 0.250 *M* steps was prepared and bromophenol blue dye (Sigma–Aldrich) was added to the mixture to provide a visual recognition of dehydrated conditions *versus* nondehydrated conditions. Prior to collecting data, the wells containing crystals were pierced with a thin blade and 30 µl of the deep-well block sodium chloride solution was added to the reservoir (Fig. 1). The resulting range of salt concentrations (0–2.5 *M*) covers a relative humidity range at 293 K from 100% to around 87.5% in steps of approximately 1.25% (Winston & Bates, 1960). For sodium chloride concentrations beyond 2.5 *M*, the reservoir solution was partially removed and completed to 60 µl with 5 *M* sodium chloride solution to the desired sodium chloride concentrations of 2.625, 3.0, 3.3 and 3.75 *M* (equivalent to relative humidities of approximately 86.87, 85, 83.5 and 81.25%, respectively). The plates were then re-sealed for equilibration to take place overnight.

Equilibrated plates were placed in the beamline I04-1 storage hotel and the six-axis CATS robot arm (Irelec; Jacquamet *et al.*, 2009) was used to present the samples into the X-ray beam path and act as the ω rotation (Lobley *et al.*, 2012). Data were collected with a PILATUS 2M detector (Dectris) for fast room-temperature data collection.

Crystals were exposed to a 50 µm beam defined using a 50 µm beam-defining aperture with an incident flux of 1.7×10^{11} photons s^{-1} and an exposure time equivalent to 1 s per degree. About 20° of rotation (from −10 to +10°) could be collected before X-ray radiation damage was observed. About 10–15 dehydration conditions could be screened per hour of synchrotron beamtime. Data were processed using the *XDS* software package (Kabsch, 2010) and the *XDS*-refined unit-cell parameters were used to monitor the effect of dehydration on the crystal. The resolution limit was not used as a criterion to follow the progress of the experiment as the crystals suffered from radiation damage when collecting at room temperature and only incomplete data were obtained.

Data for a final salt concentration in the reservoir solution ranging from 0.625 to 3.75 *M* are displayed in Fig. 2. As the salt concentration

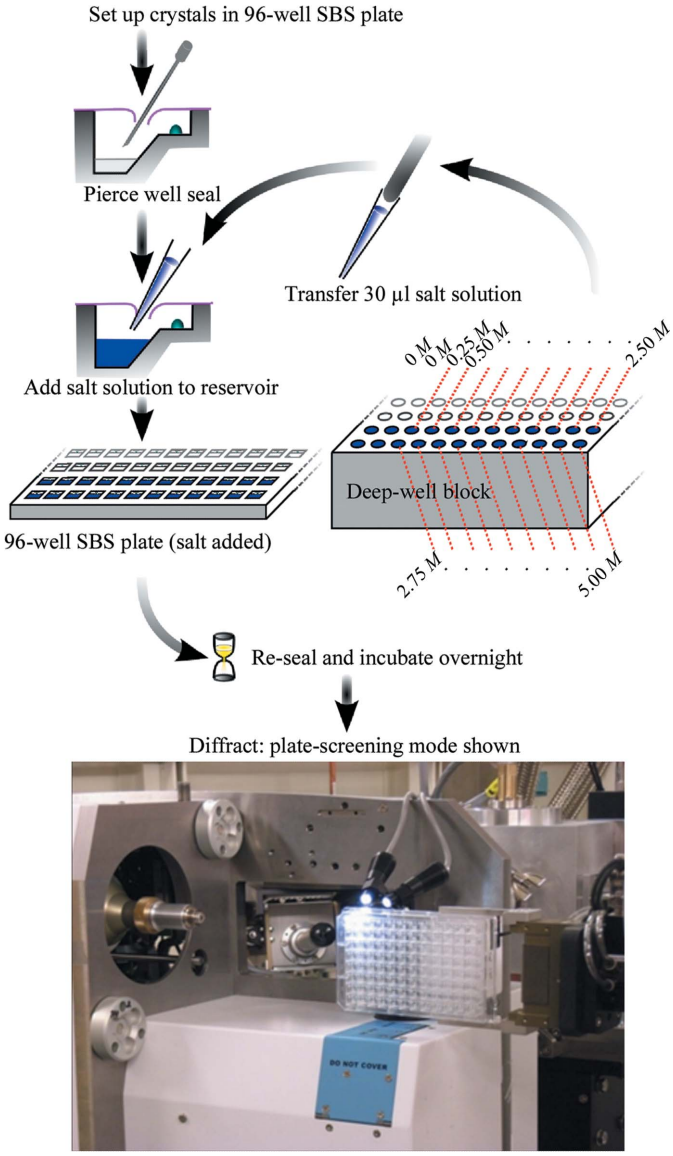

Figure 1
Steps in the dehydration experiment.

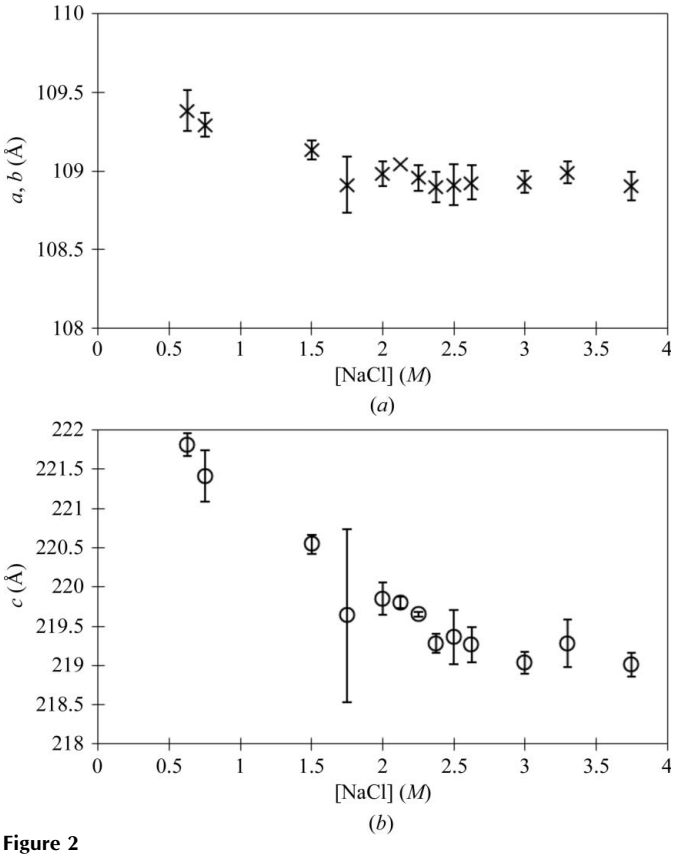

Figure 2
Effect of salt concentration on protein unit-cell parameters at 293 K: (*a*) on the *a* and *b* axes and (*b*) on the *c* axis. For each salt concentration 2–12 crystals were used for the calculation of statistics. To exclude the statistical outliers, we calculated the mean value ($\overline{x}$) for each unit-cell parameter and the corresponding standard error of the mean, σ: $\sigma = \{[\sum(x-\overline{x})^2]/n-1\}^{1/2}/n^{1/2}$, where n is the number of crystals at a single salt concentration. If one of the unit-cell parameters did not follow the rule $\overline{x}-3\sigma < x < \overline{x}+3\sigma$, the crystal was considered to be an outlier and was discarded from the final calculation of statistics. The error bar shows the standard error of the mean ($\overline{x} \pm 3\sigma$).

Table 1
Resolution and unit-cell parameters of native and dehydrated crystals.

All data sets were collected from individual crystals at 100 K. The resolution and unit-cell parameters are presented as mean values with their standard deviations in parentheses. The standard deviation is calculated using the formula $\{[\sum(x-\bar{x})^2]/(n-1)\}^{1/2}$.

Run No.	No. of data sets	[NaCl] (*M*)	High-resolution limit (Å)	Unit-cell parameters (Å) *a*	*b*	*c*
Native crystals						
Run 1	17	0	2.92 (0.15)	107.49 (0.18)	107.49 (0.18)	219.74 (1.33)
Run 2	5	0	2.91 (0.13)	107.40 (0.15)	107.40 (0.15)	221.37 (1.28)
Runs 1 and 2	22		2.92 (0.14)	107.47 (0.17)	107.47 (0.17)	220.11 (1.47)
Dehydrated crystals						
Run 1	29	2.5	2.60 (0.15)	107.43 (0.19)	107.43 (0.19)	216.87 (0.40)
Run 2	18	3.75	2.56 (0.14)	107.52 (0.19)	107.52 (0.19)	217.15 (0.32)
Runs 1 and 2	47		2.58 (0.14)	107.46 (0.19)	107.46 (0.19)	216.97 (0.39)

was increased, the unit-cell parameters for all three axes decreased. Beyond a concentration of 2.5 *M* no further changes were observed. The overall change in dimensions was greater for the *c* axis than for the *a* or *b* axes. Fig. 2(*a*) shows that the *a* and *b* axes decreased slightly from 109.4 to 108.9 Å, corresponding to an overall change of 0.5%, while the *c* axis decreased from 221.8 to 219.0 Å (1.3% overall change; Fig. 2*b*).

To characterize the effect of the unit-cell parameter shrinkage observed at room temperature, full data sets were collected from native and dehydrated crystals (22 and 47, respectively) at 100 K on beamline I04-1. Two salt concentrations, 2.5 and 3.75 *M* (around 87.5 and 81.25% relative humidity, respectively), at the start and end of the plateau region were chosen to provide a clear assessment of the effect of dehydration on crystal quality. Crystals were mounted onto cryoloops from the 96-well plates, where some drops were left untouched and others were dehydrated with sodium chloride. Native crystals, despite being grown from 2 *M* ammonium sulfate, could not be cryoprotected without the addition of 20%(*v*/*v*) ethylene glycol, while the dehydrated crystals did not require any cryoprotection. It has been previously reported that crystals can be cryoprotected without the addition of cryoprotecting agents if the surrounding solvent has been completely removed (Pellegrini *et al.*, 2011). To test reproducibility, two independent data-collection runs were carried out. Complete data sets were collected using a 70 µm beam-defining aperture with an incident flux of 3.1×10^{11} photons s^{-1} and an exposure time equivalent to 1 s per degree. Data were processed using the *xia*2 pipeline software, with the default criteria for the resolution cutoff based on a merged $\langle I/\sigma(I)\rangle$ of greater than 2 and an unmerged $I/\sigma(I)$ of greater than 1 (Winter, 2010). No remarkable change was observed in the mosaicity of the native and dehydrated samples (data not shown); however, there was an overall improvement of the Wilson *B* temperature factor for the dehydrated crystals compared with the native crystals independent of the resolution (Fig. 3). Changes in the crystal unit-cell parameters and resolution are summarized in Table 1 and all crystallographic data statistics are available in Supplementary Table S1[1]. Dehydrated crystals diffracted to an improved average resolution of 2.6 Å, with the best crystal diffracting to 2.45 Å resolution, while the native crystals diffracted to an average resolution of 2.9 Å. For both native and dehydrated crystals the standard deviation of resolution was between 0.13 and 0.15 Å, which indicates good reproducibility of the crystal diffraction power for each population. A closer look at the unit-cell parameters showed that the *a* and *b* axes are similar in the native and dehydrated crystals but the most striking change is in the *c* axis, which varies from 220.11 Å down to 216.98 Å after dehydration. It is worth noting that for both native and dehydrated crystals all unit-cell parameters for data collected at cryo-temperature are about 2 Å shorter than for the room-temperature data. The standard deviation is reproducible in both runs and, interestingly, the *c*-axis standard deviation is 1.47 Å for the native crystals but 0.39 Å for the dehydrated crystals. Under native conditions, this variation of the *c* axis might be owing to different levels of dehydration taking place while the crystals are transferred into the cryoprotectant solution and are being cryo-cooled. Conversely, dehydrated crystals benefited from the absence of an extra crystal-handling step involving transfer into cryoprotectant solution. Changes in the unit-cell parameters are represented by a small reduction of the solvent content by 1% from 61 to 60% as estimated by the Matthews coefficient calculation (Matthews, 1968). To investigate the effect of dehydration on crystal packing, we superposed the native and dehydrated crystal structures on the unit-cell origin using *CSYMMATCH* (Winn *et al.*, 2011), calculated the coordinates of the native and dehydrated centroids and the distance separating them using *LSQKAB* (Kabsch, 1976) and the root-mean-square deviation of the C_α atoms between both molecules. Native and dehydrated centroids are separated by 1.5 Å along the *c* axis, resulting in an average root-mean-square deviation of the main chain of 1.64 Å between the structures. This indicates that in the dehydrated case the molecules are packed more tightly along the *c* axis. Furthermore, initial analysis of both native and dehydrated electron density indicates that some structural rearrangements have occurred in the dehydrated case (details of the structures will be presented elsewhere).

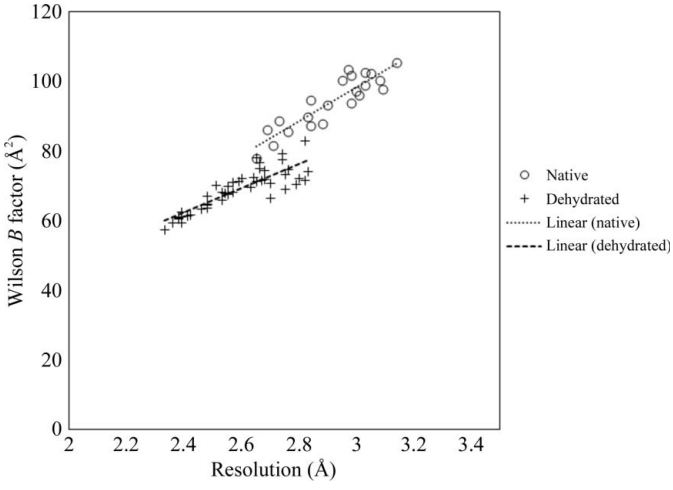

Figure 3
Distribution of the Wilson *B* temperature factor *versus* resolution. Two different trend lines in the distribution of the Wilson *B* temperature factor for the native (circles) and the dehydrated (+) crystals are observed.

3. Conclusions

Here, we have presented a simple dehydration method which relies on a small quantity of protein to prepare an SBS-format 96-well crystallization plate and on consumables commonly used in crystallization (96 deep-well blocks and bromophenol blue dye). Although sodium chloride was used as a dehydrating agent, it can easily be substituted by other salts or polyethylene glycols (Wheeler *et al.*, 2012). The method is easily implemented in the home laboratory

[1] Supplementary material has been deposited in the IUCr electronic archive (Reference: TZ5020). Services for accessing this material are described at the back of the journal.

prior to accessing an X-ray plate-screening facility (either in-house or at a synchrotron). The 96-well setup allows a range of dehydration points to be analysed at once and can also be used to assess the reproducibility of the experiment. *In situ* data collection removes the critical and potentially damaging step of manually handling the crystals and provides an objective evaluation of their quality using X-rays. We have also shown that small wedges of *in situ* data provide reliable refined unit-cell parameters that can be used to monitor the crystal-dehydration process (as currently used in humidity-control experiments).

The throughput of the plate-screening setup on beamline I04-1 would allow up to 360 conditions to be analysed per 24 h of beam-time. In this particular case the protein crystals grew reproducibly, allowing us to perform a comprehensive dehydration screen with statistical analysis in a single experiment. Prior to dehydration, the diffraction quality was consistently limited to 2.9 Å resolution. After dehydration, the crystals did not require any cryoprotectant solution and their diffraction was reproducibly improved. This improvement was by an average of 0.3 Å, with the best resolution extending as far as 2.45 Å. We expect that in the case of this protein this higher resolution structure will greatly aid in the interpretation of its biological function.

We are currently evaluating whether this simple and fast procedure can be routinely extended to other systems such as membrane proteins, protein complexes and delicate systems that require volatile compounds for their stability.

The authors would like to thank Dr Martin Walsh for providing the initial crystals, Dr Marco Mazzorana for practical suggestions for the experimental setup, Dr David Waterman for his advice on statistical data handling, Dr Alex Cameron for reading the manuscript and the Membrane Protein Laboratory (MPL). MPL is supported by Welcome Trust grant No. 062164/Z/00.

References

Axford, D. *et al.* (2012). *Acta Cryst.* D**68**, 592–600.
Bingel-Erlenmeyer, R., Olieric, V., Grimshaw, J. P. A., Gabadinho, J., Wang, X., Ebner, S. G., Isenegger, A., Schneider, R., Schneider, J., Glettig, W., Pradervand, C., Panepucci, E. H., Tomizaki, T., Wang, M. & Schulze-Briese, C. (2011). *Cryst. Growth Des.* **11**, 916–923.
Efremov, R. G., Baradaran, R. & Sazanov, L. A. (2010). *Nature (London)*, **465**, 441–445.
Hargreaves, D. (2012). *J. Appl. Cryst.* **45**, 138–140.
Heras, B. & Martin, J. L. (2005). *Acta Cryst.* D**61**, 1173–1180.
Jacquamet, L., Joly, J., Bertoni, A., Charrault, P., Pirocchi, M., Vernede, X., Bouis, F., Borel, F., Périn, J.-P., Denis, T., Rechatin, J.-L. & Ferrer, J.-L. (2009). *J. Synchrotron Rad.* **16**, 14–21.
Jacquamet, L., Ohana, J., Joly, J., Legrand, P., Kahn, R., Borel, F., Pirocchi, M., Charrault, P., Carpentier, P. & Ferrer, J.-L. (2004). *Acta Cryst.* D**60**, 888–894.
Kabsch, W. (1976). *Acta Cryst.* A**32**, 922–923.
Kabsch, W. (2010). *Acta Cryst.* D**66**, 125–132.
Kiefersauer, R., Than, M. E., Dobbek, H., Gremer, L., Melero, M., Strobl, S., Dias, J. M., Soulimane, T. & Huber, R. (2000). *J. Appl. Cryst.* **33**, 1223–1230.
Lobley, C. M. C., Aller, P., Douangamath, A., Reddivari, Y., Bumann, M., Bird, L. E., Nettleship, J. E., Brandao-Neto, J., Owens, R. J., O'Toole, P. W. & Walsh, M. A. (2012). *Acta Cryst.* F**68**, 1427–1433.
Maire, A. le, Gelin, M., Pochet, S., Hoh, F., Pirocchi, M., Guichou, J.-F., Ferrer, J.-L. & Labesse, G. (2011). *Acta Cryst.* D**67**, 747–755.
Matthews, B. W. (1968). *J. Mol. Biol.* **33**, 491–497.
Mueller, U., Darowski, N., Fuchs, M. R., Förster, R., Hellmig, M., Paithankar, K. S., Pühringer, S., Steffien, M., Zocher, G. & Weiss, M. S. (2012). *J. Synchrotron Rad.* **19**, 442–449.
Newman, J. (2006). *Acta Cryst.* D**62**, 27–31.
Pellegrini, E., Piano, D. & Bowler, M. W. (2011). *Acta Cryst.* D**67**, 902–906.
Russi, S., Juers, D. H., Sanchez-Weatherby, J., Pellegrini, E., Mossou, E., Forsyth, V. T., Huet, J., Gobbo, A., Felisaz, F., Moya, R., McSweeney, S. M., Cusack, S., Cipriani, F. & Bowler, M. W. (2011). *J. Struct. Biol.* **175**, 236–243.
Russo Krauss, I., Sica, F., Mattia, C. A. & Merlino, A. (2012). *Int. J. Mol. Sci.* **13**, 3782–3800.
Sanchez-Weatherby, J., Bowler, M. W., Huet, J., Gobbo, A., Felisaz, F., Lavault, B., Moya, R., Kadlec, J., Ravelli, R. B. G. & Cipriani, F. (2009). *Acta Cryst.* D**65**, 1237–1246.
Soliman, A. S. M., Warkentin, M., Apker, B. & Thorne, R. E. (2011). *Acta Cryst.* D**67**, 646–656.
Umena, Y., Kawakami, K., Shen, J. R. & Kamiya, N. (2011). *Nature (London)*, **473**, 55–60.
Wheeler, M. J., Russi, S., Bowler, M. G. & Bowler, M. W. (2012). *Acta Cryst.* F**68**, 111–114.
Winn, M. D. et al. (2011). *Acta Cryst.* D**67**, 235–242.
Winston, P. W. & Bates, D. H. (1960). *Ecology*, **41**, 232.
Winter, G. (2010). *J. Appl. Cryst.* **43**, 186–190.